

Identification of optical transitions in cubic and hexagonal GaN by spatially resolved cathodoluminescence

J. Menniger, U. Jahn, O. Brandt, H. Yang, and K. Ploog

Paul-Drude-Institut für Festkörperelektronik, Hausvogteiplatz 5-7, D-10117 Berlin, Germany

(Received 14 July 1995)

The hexagonal and cubic phases of GaN are characterized by spatially resolved cathodoluminescence (CL) spectra from micrometer-size single crystals with either hexagonal or cubic *habits* grown by plasma-assisted molecular-beam epitaxy. At 5 K, distinct narrow excitonic lines are found at 3.472 and 3.272 eV for the hexagonal and cubic phase, yielding energy gaps of 3.500 and 3.300 eV, respectively. Detailed temperature- and intensity-dependent CL measurements on cubic GaN crystals enable us to clearly identify the exciton (free: 3.272 eV, bound: 3.263 eV) and the donor-acceptor pair (3.150 eV) transition. Moreover, we determine the donor-band and acceptor-band transition energy for this phase. In addition, phonon replicas of the exciton line and of the donor-acceptor pair transition are observed at 3.185 and 3.064 eV, respectively.

GaN is a direct wide band-gap semiconductor, which is important for future applications in optoelectronics. The equilibrium structure of GaN is wurtzite (hexagonal). In the past few years, it has been demonstrated that it is possible to produce layers of the metastable zinc-blende (cubic) phase.¹⁻⁸ However, the results reported on band-gap energy (E_g) and luminescence transitions of nominally cubic (*c*) GaN layers are inconsistent with each other. The optical properties of hexagonal (*h*) GaN were investigated in detail in the early seventies by Dingle *et al.*,^{9,10} Lagerstedt and Monemar,¹¹ and Monemar,¹² resulting in a value for the energy gap E_g (*h*-GaN) of 3.503 eV at 1.6 K. Theoretical calculations¹³⁻¹⁵ predict that *c*-GaN has a slightly lower gap than *h*-GaN. The predicted differences between E_g (*h*-GaN) and E_g (*c*-GaN) range from 100 meV (Ref. 13) to 400 meV (Ref. 14). Optical absorption and photoreflectance experiments have provided values of E_g (*c*-GaN) between 3.270 and 3.300 eV at 10 K.^{3,4,16} However, larger differences are found among the reported cathodoluminescence (CL) and photoluminescence (PL) spectra.^{2,5-7} The discrepancies in the luminescence results may originate from fractions of *h*-GaN interspersed in nominal *c*-GaN layers.^{2,6}

The aim of this work is to provide clearly separated CL spectra of nominally undoped *h*-GaN and of *c*-GaN. We use spatially resolved CL taken from micrometer-size GaN crystals, which exhibit hexagonal or cubic *habits*, to distinguish the CL of the two phases.

The samples are grown by solid-source molecular-beam epitaxy (MBE) on GaAs (001) substrates, employing a dc plasma discharge source for exciting molecular N_2 to atomic N and to N_2 ions. Growth of GaN is initiated at 630–680 °C under nearly stoichiometric conditions, using a slow growth rate (0.05 ML/s). After establishing a smooth, cubic GaN layer as revealed by reflection high-energy electron diffraction, the Ga flux is increased by a factor of 4. Then Ga droplets evolve at the growth front, giving rise to a vapor-liquid solidlike growth of GaN crystals inside the droplets. After growth is completed, the samples are treated with concentrated HCl to remove liquid Ga and thus give access to the GaN crystals on the surface of a 1- μ m-thick GaN layer. These crystals, having sizes in the micrometer range, exhibit

smooth facets characteristic for either the zinc-blende or wurtzite structure and are single crystals as determined by transmission electron-diffraction patterns. The CL experiments are carried out in a scanning electron microscope (SEM) equipped with an Oxford Mono-CL and He cooling stage system providing a continuous temperature control ranging from 5–300 K. The electron-beam energy amounts to 5 keV and the current is usually set to about 0.1 nA. A grating monochromator and a cooled photomultiplier are used in conjunction with a conventional photon counting technique to disperse and detect the CL, respectively. The surface morphology of the GaN samples is monitored by (SE) images.

Figure 1 shows a SE micrograph of several GaN single crystals grown by the MBE procedure described above. Two of these crystals exhibit the distinct hexagonal growth *habit*. All six angles of the top plane of the truncated pyramids are

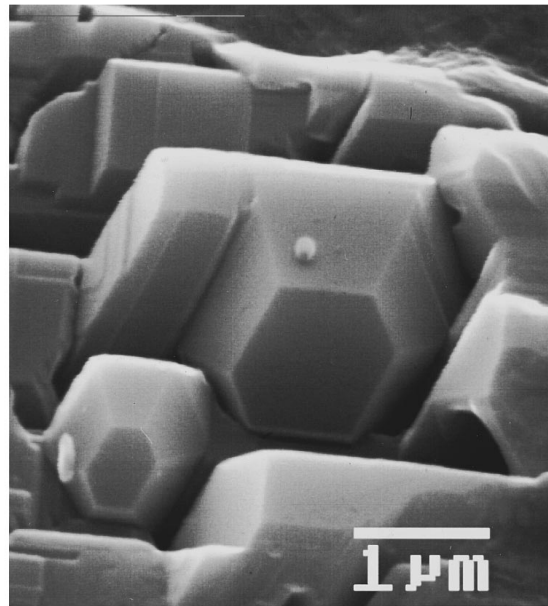


FIG. 1. Secondary electron micrograph of GaN single crystals grown by molecular-beam epitaxy.

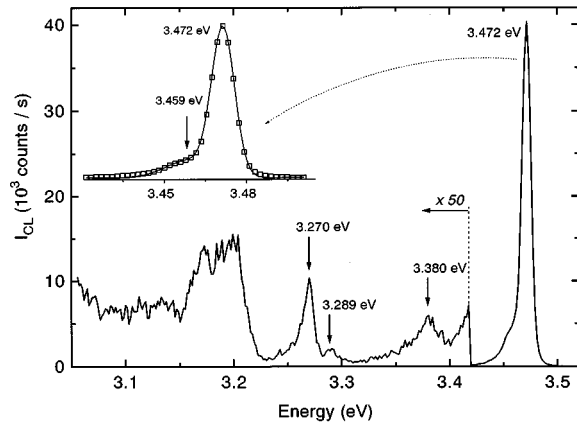


FIG. 2. Cathodoluminescence spectrum of a hexagonal GaN crystal recorded at 5 K. In the inset, the full line is a fit to the data points using two Gaussians with line positions at 3.459 and 3.472 eV. The FWHM of the main line amounts to 10 meV.

determined to be 120° . Since they are tilted with respect to the sample plane, the perspective of the SE image has to be taken into account to estimate these angles. Additional cubic crystals identified by their square facets surround these hexagonal crystals.

CL in connection with SEM allows us to position the electron beam accurately either on a cubic or on a hexagonal crystal. Consequently, a separate excitation of the cubic and hexagonal phase is possible. A CL spectrum from the hexagonal crystal is shown in Fig. 2. This CL spectrum exhibits an intense, narrow line at 3.472 eV with a full width at half maximum (FWHM) of 10 meV and a series of weak lines below 3.400 eV. The main line actually consists of two lines centered at 3.472 and 3.459 eV (cf. inset of Fig. 2). The CL line positions in this spectrum are compiled in Table I together with corresponding data obtained by Dingle *et al.*⁹ and Lagerstedt and Monemar.¹¹

Comparing our results with those reported in Refs. 9 and 11 shows that the strong CL line at 3.472 eV is due to radiative transitions of both bound excitons (neutral donor) and free excitons (cf. Refs. 11 and 12). The line at about 3.459 eV, which is not well resolved, can be related to the exciton bound to a neutral acceptor. The weak lines at 3.380 and 3.289 eV are most probably phonon replicas of the strong exciton line. The CL band at 3.270 eV can be the donor-acceptor pair transition as recently confirmed by Glaser *et al.*¹⁷ or might originate from the cubic phase surrounding the hexagonal crystals (see below).

Our CL results show that the excitonic transition energy

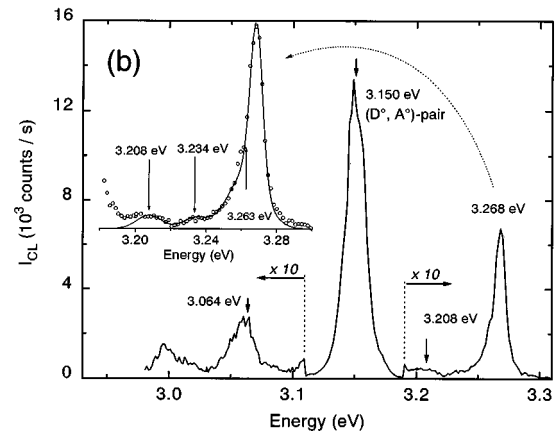
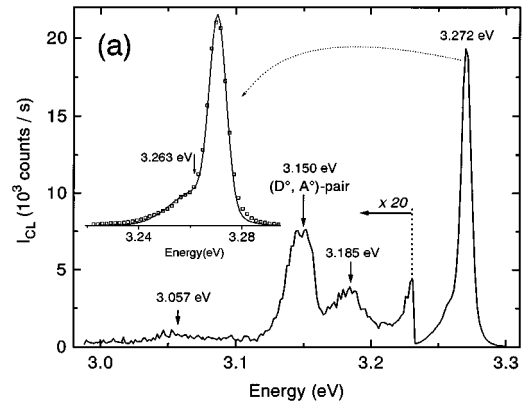


FIG. 3. Cathodoluminescence spectra of a cubic GaN crystal recorded at 5 K. For (a) and (b), a different excitation position was chosen on the same crystal. The solid lines in the insets of (a) and (b) are fits to the data points, using two and four Gaussians, respectively. The FWHM of the exciton line amounts to 8 meV (a) and 11 meV (b).

of a micrometer-size hexagonal GaN crystal agrees well with that of 100–250- μm -thick layers.⁹ Recently, Shan *et al.*¹⁸ published values obtained from thinner (4.2- μm -thick) *h*-GaN layers, which are systematically higher by 10 meV. The reason for this discrepancy is probably related to strain effects. In fact, Namiwae *et al.*¹⁹ have shown that the exciton line position of *h*-GaN layers increases by about 10 meV when the thickness is reduced from 300 to 20 μm .

When the CL excitation position is set on a cubic shaped GaN crystal, we obtain spectra as shown in Figs. 3(a) and 3(b). The two spectra are taken from the same cubic crystal, but recorded at different locations. Both spectra exhibit CL

TABLE I. Peak energy positions (in eV) of the CL spectra recorded on *h*-GaN crystals at 5 K compared with PL results from *h*-GaN layers reported by Dingle *et al.* (Ref. 9) and Lagerstedt and Monemar (Ref. 11). FX is the free exciton, (D^0, X) the exciton bound to a neutral donor, (A^0, X) the exciton bound to a neutral acceptor, and (D^0, A^0) the donor-acceptor pair transition, respectively, LO_{X1} and LO_{X2} are phonon replicas.

	FX	(D^0, X)	(A^0, X)	LO_{X1}	LO_{X2}	(D^0, A^0)
This work		3.472	3.459	3.380	3.289	
Dingle <i>et al.</i> (Ref. 9)	3.474	3.466–3.468	3.455	3.380	3.290	3.257
Lagerstedt (Ref. 11)	3.475	3.469	3.454	3.377		3.263

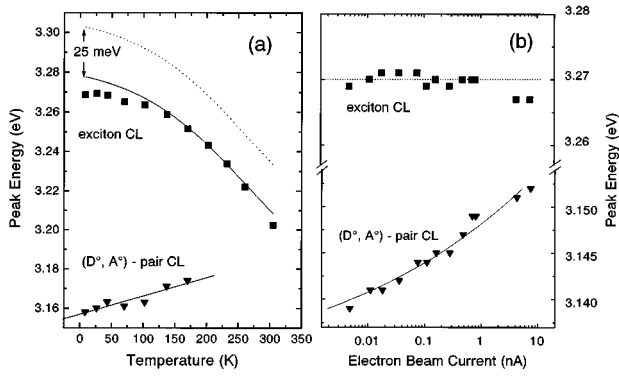


FIG. 4. Temperature (a) and intensity (b) dependence of the line positions of the excitonic (rectangles) and (D^0, A^0) -pair (triangles) emission obtained from a cubic GaN crystal. The excitation intensity used in (a) corresponds to an electron-beam current of about 10 nA. The temperature in (b) is 5 K. The straight line in (a) is a least-squares fit to the data points (triangles). The full line related to the rectangles in (a) is the downwards shifted temperature dependence of the band-gap energy according to Ref. 16 (dotted line). The full line in (b) is a least-squares fit of the data points (triangles) to Eq. (1) with values of E_∞ and E_D of 3.125 eV and 75 meV, respectively. The dotted line is a guide to the eye.

lines at almost identical energetic positions, but the intensity ratios between these lines vary sensitively with the spot position. First, we discuss the line around 3.270 eV, which varies in its spectral position between 3.268 and 3.272 eV for different excitation locations on the crystal. Since we do not find any other CL line at higher energies on our cubic crystals, this luminescence is assigned to the lowest excitonic transition of cubic GaN. Figures 4(a) and 4(b) show the temperature (T) and intensity (I) dependence of the line positions of the near band-edge CL, respectively. In both graphs the full rectangles represent the excitonic transition. For $T > 100$ K, the line energy (E_p) approaches the temperature dependence of the band-gap energy (E_g) of cubic GaN according to Ramírez-Flores *et al.*¹⁶ When the excitation density (electron-beam current) is changed [cf. Fig. 4(b)], we do not observe any variation of E_p as expected for an excitonic

transition.¹⁹ The deviation of $E_p(T)$, with respect to the downwards shifted curve $E_g(T)$ between 5 and 100 K and their coincidence with increasing T [cf. Fig. 4(a)], indicate that, for low T , the excitonic CL is mainly due to bound excitons at the excitation location, whereas the free exciton dominates for higher T . For $T > 100$ K, the good agreement between the downwards shifted $E_g(T)$ and the data points suggests an exciton binding energy E_x of 25 meV for cubic GaN, which is close to the value of 28 meV found by Dingle *et al.*⁹ and Monemar¹² for the hexagonal phase.

The second distinct CL line (at 3.150 eV) becomes dominant at excitation spots on the cubic crystal, where the intensity of the excitonic line is decreased. The temperature and intensity dependence of the corresponding line energy (E_{DA}) is presented in Figs. 4(a) and 4(b) as full triangles, respectively. With both T and I , E_{DA} increases as expected for donor-acceptor (D^0, A^0) -pair transitions.^{20,21} For weakly compensated semiconductors, an increase of E_{DA} of a few meV is expected, when I is increased by a factor of 10. The intensity dependence of E_{DA} can then be written as²⁰

$$I \propto \frac{\{(E_{DA} - E_\infty)^3 \exp[-2E_D/(E_{DA} - E_\infty)]\}}{(E_D + 2E_\infty - 2E_{DA})}, \quad (1)$$

where $E_\infty = E_g - (E_A + E_D)$, with E_D and E_A denoting the donor and acceptor binding energies, respectively. In Fig. 4(b), the solid line through the data points of E_{DA} is a least-square fit to the experimental points using Eq. (1), which results in values for E_∞ and E_D of 3.125 eV and 75 meV. Compared to the experimentally found (D^0, A^0) line position at 3.150 eV, these values are reasonable, indicating the validity of Eq. (1) for our cubic GaN crystals. Consequently, we used the values of the fitting parameters E_∞ and E_D to estimate the acceptor binding energy resulting in $E_A = 100$ meV, when the band-gap energy of cubic GaN is assumed to be $E_g = 3.300$ eV.¹⁶

The important result is that the (D^0, A^0) -pair transition is closer in energy to the fundamental excitonic transition for cubic than for hexagonal GaN.^{10,11,17} The cubic phase should thus exhibit not only a shallow donor, but also a quite shallow acceptor state, as predicted by the above fitting proce-

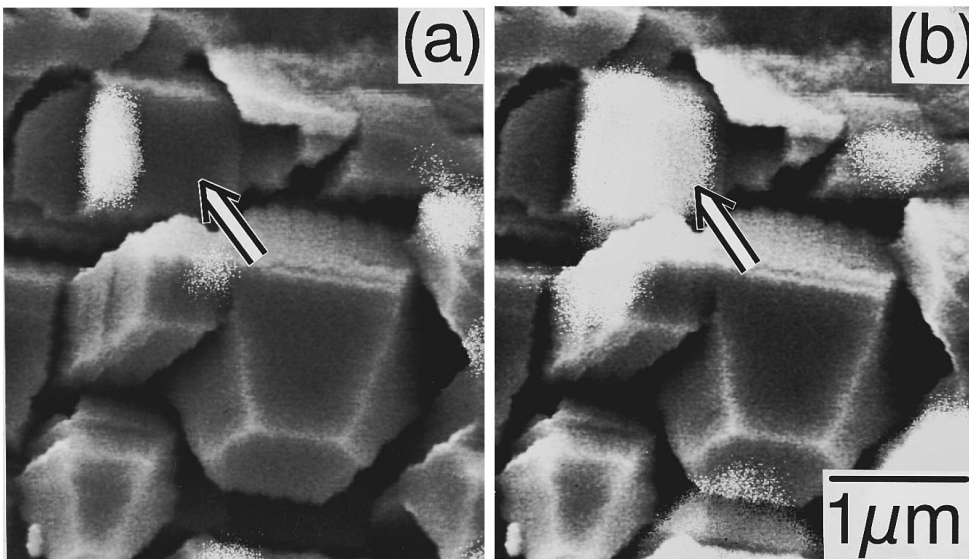


FIG. 5. Secondary electron micrograph of the crystals in Fig. 1 superimposed by CL micrographs recorded at the detection energy of the cubic fundamental exciton and (D^0, A^0) -pair transition in (a) and (b), respectively. The crystal of interest is marked by arrows.

TABLE II. Peak energy positions (in eV) of the CL spectra recorded on *c*-GaN crystals at 5 K, FX, BX, (D^0, h), (A^0, e), and (D^0, A^0) are the free exciton, bound exciton, donor-band, and acceptor-band transitions, respectively. LO_x and LO_{DA} are the phonon replicas of the exciton and (D^0, A^0)-pair transitions.

FX	BX	(D^0, h)	(A^0, e)	(D^0, A^0)	LO_x	LO_{DA}
3.272	3.263	3.234	3.208	3.150	3.185	3.064

ture. Indeed, in the case of the strong (D^0, A^0)-pair CL, we can recognize two additional weak CL lines between the excitonic and (D^0, A^0)-pair CL lines [cf. inset of Fig. 3(b)]. We assign the lines at 3.234 and 3.208 eV tentatively to free to bound transitions involving the neutral donor and acceptor level, respectively, yielding donor and acceptor binding energies of $E_D=68$ and $E_A=94$ meV, respectively. The values of this set of binding energies are close to the predicted ones ($E_D=75$ meV and $E_A=100$ meV), which demonstrates good agreement within the experimental uncertainty. Note that, when following Haynes rule,²² the binding energy of excitons bound to both the donor and acceptor are estimated to be of the order of 10 meV. This value is consistent with the more pronounced low-energy broadening and the shift to lower energy of the excitonic line in Fig. 3(b) compared with that in Fig. 3(a).

The energy of the emitted photons related to the (D^0, A^0) pair is

$$E_{DA} = E_g - (E_A + E_D) + \frac{e^2}{\epsilon r}, \quad (2)$$

where ϵ is the dielectric constant and r the spatial pair separation. The last term arises from the Coulomb interaction of the carriers. With $E_g=3.300$ eV, we obtain a value of 12 meV for this term, which agrees rather well with the value assumed in Ref. 11 for hexagonal GaN.

Finally, the CL lines at 3.185 and 3.064 eV in Figs. 3(a) and 3(b), respectively, exhibit one common feature: Their spectral separation from the main CL line [exciton in (a) and (D^0, A^0) pair in (b)] amounts in both cases to 86 meV, suggesting that they are due to LO-phonon replicas of the respective transition.

The strong spatial inhomogeneity of the (D^0, A^0)-pair CL intensity and the correlated variation of the excitonic CL indicates that the defects or impurities forming (D^0, A^0) pairs are inhomogeneously distributed within the cubic GaN crystals. Similar phenomena were observed by Kawarada *et al.*,²³ in the case of small diamond particles and are presumably related to impurity or defect segregation. Figure 5 shows a SE micrograph of the crystals (cf. Fig. 1) superim-

posed by CL images recorded at the exciton (a) and (D^0, A^0)-pair (b) transition energy. The distinct bright regions on top of the cubic crystal marked by arrows, which change in position and shape between (a) and (b), reflect the spatial CL intensity distribution, demonstrating that the CL originates from different crystal facets, when the detection energy is switched between the excitonic and (D^0, A^0)-pair transition.

The identification of optical transitions from cubic GaN is often made more difficult by the inferior quality of the GaN layers. Factors responsible for this may include phase mixing, extended defects, and residual inhomogeneous strain. Therefore, the photon energies of luminescence lines ascribed to specific transitions for nominally cubic GaN vary considerably between different authors. Values for the cubic band-gap energy deduced from absorption, reflectance, and from photoreflectance data scatter around a value of 3.300 eV at $T \leq 10$ K. Perhaps, the most accurate results were presented by Ramírez-Flores *et al.*,¹⁶ who obtained $E_g=(3.302 \pm 0.004)$ eV. Our results concerning cubic GaN are summarized in Table II. The exciton CL line energy for cubic GaN is determined to be 3.272 eV. This is the highest value measured for different excitation locations. Taking into account an E_x of 25–28 meV, E_g (cubic) is estimated to be 3.297–3.300 eV, which is in excellent agreement with the work of Ramírez-Flores *et al.* Hence, we conclude that the band-gap energy of our crystals is not shifted noticeably by strain. Therefore, the CL spectra of Figs. 2 and 3 are representative of optical transitions of unstrained hexagonal and cubic GaN, respectively. Moreover, we determine the bound exciton, the donor-band, the acceptor-band, and donor-acceptor pair transition energies of cubic GaN to be 3.263, 3.234, 3.208, and 3.150 eV, respectively.

The authors would like to thank A. Trampert for transmission electron microscopy, G. Jungk and H. Raidt for helpful discussions, and H. T. Grahn for a critical revision of the manuscript. Part of this work was supported by the Bundesministerium für Bildung und Wissenschaft of the Federal Republic of Germany.

¹M. J. Paisley, Z. Sitar, J. B. Posthill, and R. F. Davis, *J. Vac. Sci. Technol. A* **7**, 701 (1989).

²S. Strite, J. Ruan, Z. Li, A. Salvador, H. Chen, D. J. Smith, W. J. Choyke, and H. Morkoç, *J. Vac. Sci. Technol. B* **9**, 1924 (1991).

³T. Lei, T. D. Moustakas, R. J. Graham, Y. He, and S. J. Berkowitz, *J. Appl. Phys.* **71**, 4933 (1992).

⁴R. C. Powell, N. E. Lee, Y. W. Kim, and J. E. Greene, *J. Appl. Phys.* **73**, 189 (1993).

⁵H. Liu, A. C. Frenkel, J. G. Kim, and R. M. Park, *J. Appl. Phys.* **74**, 6124 (1993).

⁶H. Okumura, S. Yoshida, and T. Okahisa, *Appl. Phys. Lett.* **64**, 2997 (1994).

⁷C. H. Hong, D. Pavlidis, S. W. Brown, and S. C. Rand, *J. Appl. Phys.* **77**, 1705 (1995).

⁸T. S. Cheng, L. C. Jenkins, S. E. Hooper, C. T. Foxon, J. W. Orton, and D. E. Lacklison, *Appl. Phys. Lett.* **66**, 1509 (1995).

- ⁹R. Dingle, D. D. Sell, S. E. Stokowski, and M. Ilegems, *Phys. Rev. B* **4**, 1211 (1971).
- ¹⁰R. Dingle and M. Ilegems, *Solid State Commun.* **9**, 175 (1971).
- ¹¹O. Lagerstedt and B. Monemar, *J. Appl. Phys.* **45**, 2266 (1974).
- ¹²B. Monemar, *Phys. Rev. B* **10**, 676 (1974).
- ¹³S. Bloom, G. Harbeke, E. Meier, and I. B. Ortenburger, *Phys. Status Solidi B* **66**, 161 (1974).
- ¹⁴B. J. Min, C. T. Chan, and K. M. Ho, *Phys. Rev. B* **45**, 1159 (1992).
- ¹⁵A. Rubio, J. L. Corkill, M. L. Cohen, E. L. Shirley, and S. G. Louie, *Phys. Rev. B* **48**, 11 810 (1993).
- ¹⁶G. Ramírez-Flores, H. Navarrow-Contreras, Lastras-Martinez, R. C. Powell, and J. E. Greene, *Phys. Rev. B* **50**, 8433 (1994).
- ¹⁷E. R. Glaser, T. A. Kennedy, K. Doverspike, L. B. Rowland, D. K. Gaskill, J. A. Freitas, M. A. Khan, D. T. Olson, J. N. Kuznia, and D. K. Wickenden, *Phys. Rev. B* **51**, 13 326 (1995).
- ¹⁸W. Shan, T. J. Schmidt, X. H. Yang, S. J. Hwang, J. J. Song, and B. Goldenberg, *Appl. Phys. Lett.* **66**, 985 (1995).
- ¹⁹K. Naniwae, S. Itoh, H. Amano, K. Itoh, K. Hiramatsu, and I. Akasaki, *J. Cryst. Growth* **99**, 381 (1990).
- ²⁰L. Pavesi and M. Guzzi, *J. Appl. Phys.* **75**, 4779 (1994).
- ²¹P. J. Dean and J. L. Merz, *Phys. Rev.* **178**, 1310 (1969).
- ²²J. R. Haynes, *Phys. Rev. Lett.* **4**, 361 (1960).
- ²³H. Kwarada, Y. Yokota, Y. Mori, K. Nishimura, and A. Hiraki, *J. Appl. Phys.* **67**, 983 (1990).